Lasers in Manufacturing Conference 2023

Ultrashort pulse laser phase transition of 2D MoS_2 produced by atomic layer deposition

Malte J. M. J. Becher[a,*], Leander Willeke[b], Martin Wilken[c], Anjana Devi[c], Claudia Bock[b] and Andreas Ostendorf[a]

[a]*Applied Laser Technologies, Ruhr University Bochum, Universitätsstraße 150, 44801 Bochum, Germany*
[b]*Microsystems Technology, Ruhr University Bochum, Universitätsstraße 150, 44801 Bochum, Germany*
[c]*Inorganic Materials Chemistry, Ruhr University Bochum, Universitätsstraße 150, 44801 Bochum, Germany*

Abstract

2D materials like transition metal dichalcogenides (TMDCs) are promising for flexible electronic devices. Two-dimensional molybdenum disulfide (2D MoS_2), with a two-phase system consisting of a semiconductor phase (2H) with a tunable bandgap up to 1,8 eV and a metastable metallic phase (1T), provide the possibility of in plane edge contacts with low contact resistance. By using ultrashort pulse (usp) lasers, a phase transition from the 1T to the 2H phase is possible. In addition, due to the 'cold' energy input, more flexible and temperature-sensitive substrates can be used. In this study MoS_2 films were deposited by atomic layer deposition (ALD) on SiO_2/Si and flexible glass wafers, intercalated with lithium and processed with an NIR fs-laser (λ = 1030 nm, t = 400 fs) with scanning speeds up to v = 10 mm/s. Raman Spectroscopy is used to confirm the phase transition and investigate the effect of the transformation on the electrical resistance of the MoS_2 layer.

Keywords:

1. Introduction

2D materials have gained growing interest in the research field since the exfoliation of graphene in. Since then, the field of 2D materials has grown strongly and new material groups like transition metal dichalcogenides (TMDC), hexagonal boron nitride, black phosphorous and others were successful exfoliated (Novoselov et al. 2016). TMDCs, especially MoS_2, have the special properties of a tuneable bandgap (1.3 eV – 1.8 eV), with an energy gap, that can be used for electronic devices. In combination with the other outstanding mechanical and optoelectrical properties, MoS_2 is a promising material for flexible electronics and a substitute for silicon as a semiconductor material (Wang et al. 2012). For an industrial usage direct, large area deposition, a high

* Correspinding author. Tel.: +49 23432-23931
E-mail address: malte.becher@rub.de

yield and fast post treatment methods are necessary. Because of the temperature sensibility, high temperature deposition methods like chemical vapor deposition are not suitable for flexible substrates. Deposition temperatures in atomic layer deposition (ALD) as low as 100°C have been reported, making the process suitable for a direct material deposition on flexible substrates like thin glass or polymers (Neubieser et al. 2022, Jagosz et al. 2022).

Lowering contact resistance is one central key issue in improving TMDC device performance. In nature MoS_2 occurs in the stable, semiconducting, trigonal prismatic D_{3h} phase (2H), but it also has a metastable, metallic, octahedral O_h phase (1T). The in-plane phase-change contacts, refer to the use of multiple phases of a two-dimensional material for different parts of a device. The semiconductor phase acts as a channel, the metal phase acts as an electrode, and the two phases are connected by chemical bonds in a seamless manner. While, for conventional metal-TMDC contacts several effects e.g., fermi-level pinning, diffusion occur, which lead to a high contact resistance (McDonell et al. 2014, Schulman et al. 2018), these effects become much less relevant for phase-change contacts as they happen between two metals with much better conductivity than the semiconducting 2H MoS_2. It was already demonstrated for exfoliated MoS_2 flakes that phase engineering can markedly reduce the contact resistance between the source/drain electrodes and the channel to enable high-performance transistors (Kappera et al. 2014).

During the last years the intercalation of MoS_2 with lithium as an electron donor was established to transform the natural occurring 2H MoS_2 into the 1T phase (Py and Haering 1983, Xiao et al. 2019). For the retransition from the 1T into the 2H phase different strategies have been researched, including simply heating the whole film and using plasma, electron beam or laser treatments (Xiao et al. 2019). The advantages of laser processing (free forming, selective energy input, low process requirements, scalability) and especially the 'cold' energy input through ultrashort pulse (usp) lasers, makes this technique suitable for the processing of materials on flexible, temperature sensible substrates like thin glass or polymers.

First phase transformation of 1T MoS_2 into the 2H phase with the usage of continuous wave (cw) laser was described by Papadopoulos et al. 2018 and Fan et al. 2015. Also, in 2015 Guo et al. describe a femtosecond (fs) laser phase transformation process of exfoliated MoS_2 flakes with scanning speeds of 0,01 mm/s.

In this study we present a fast usp laser process, to engineer the metallic 1T into the semiconducting 2H phase of large area atomic layer deposited MoS_2 on SiO_2/Si and as well on glass wafer. We investigate the influence of the processing atmosphere, the laser fluence and the scanning speed on the phase transition. Our process involves the atomic layer deposition on 200 mm wafer and a fast usp laser process and shows a strategy towards a reliable industrial production beyond the laboratory scale.

2. Methods

2.1. Atomic layer deposition of MoS_2

The thin MoS_2 layers were prepared by use of a plasma enhanced atomic layer deposition (PEALD) process on 200 mm glass wafers (AF32eco) and SiO2/Si wafers (Jagosz et al. 2022). The SiO_2 was generated via thermal oxidation has a layer thickness of 200 nm. Bis(t-butylimido)bis(dimethylamino)molybdenum is used as a precursor with a plasma mixture of Argon (Ar) and hydrogen sulfide gas as a reactant. In the ALD alternating phases of precursor dosing and application of reactant are separated by vacuum periods. Thus, a complete self-limiting surface coverage of precursor molecules is followed by a phase where the H_2S plasma energy leads to ligand separation and formation of polycrystalline MoS_2 layers (Jagosz et al. 2022). 150 ALD cycles result in an average MoS_2 thickness of 8.2 nm (11.7 nm) on SCHOTT AF 32® eco glass wafer (SiO_2/Si wafer).

The thickness was determined by spectroscopic ellipsometry (SENTECH Instruments GmbH, Model SE800 DUV).

2.2. Phase transformation 2H to 1T of MoS_2

To induce the phase transformation from the 2H into the 1T phase the lithium intercalation method was used (Py and Haering 1983). MoS_2 samples (20mm x 20 mm and 15 mm x 15 mm dimension) were inserted in 20 ml of a 1.6 mol/l n-butyllithium solution in hexane (Sigma Aldrich) for 48 hours. These phase transition experiments were performed in an argon filled Glovebox (<1ppm O_2 and H_2O; GS Glovebox Systemtechnik GmbH). After that the samples were first rinsed with hexane and afterwards rinsed with 99,9 % isopropanol.

2.3. Usp laser processing of 1T MoS_2

A femtosecond laser system from Jenoptik (JenLas D2.fs , λ = 1030 nm, τ_P = 400 fs) with a repetition rate of f_{rep} = 200 kHz was used for the phase transformation experiments. The laser fluence was adjusted with 9.3 mJ/cm² < F_P < 166.7 mJ/cm² by a half-waveplate and a polarization beam splitter. The laser beam is led to a galvanometer scanner and focused on the sample surface with a F-Θ lens, with a beam radius $\omega_0 \geq 13.1$ µm. The MoS_2 films were processed under natural atmosphere and argon flow (flow rate Q = 5 l/min). For the laser fluence the peak fluence F_P was calculated after equation 1, with the pulse energy E_P and the average laser power P_L.

$$F_P = \frac{2\,E_P}{\pi\ {\omega_0}^2} \qquad (1)$$

$$with\ E_p = \frac{P_L}{f_{rep}}$$

2.4. Sample preparation

For characterization of the layers' resistance a measurement on 20 mm x 20 mm samples of both substrates was performed with a four-point probe (4PP, Signatone Pro4) station. Additionally, a fabrication of square 70 µm x 70 µm test structures was undertaken on an SiO_2/Si sample. The here applied van-der-Pauw method gives values for the sheet resistance of test structures of arbitrary shape (van der Pauw 1958). The test structures were defined by conventional UV lithography and patterned within a SF_6 plasma. After phase transition as described above, USP laser retransformation was performed outside the contact areas and the metal contacts on top of the 1T phase are prepared via UV lithography, e-beam evaporation, and lift-off technique. The metal stack consists of a 3 nm thick Ni adhesion layer and a 70 nm thick gold layer. Finally, an epoxy resin coating was used to prevent a degradation of the film during the van-der-Pauw measurements.

2.5. Raman spectroscopy

Raman measurements were performed with a Renishaw InVia microscope (λ = 532 nm) with a laser power $P_L \leq 2$ mW and an exposure time t_E = 10 s. Unless otherwise noted, all Raman spectra are averages of

9 measurements taken at different locations on the measured sample. For the evaluation of the Raman spectra the characteristic MoS_2 peaks were fitted with a Lorentzian fit.

3. Results and discussion

The ALD process is used to deposit polycrystalline 2H MoS_2 on 200 mm SiO_2/Si and glass wafers. As seen in Figure 1 the characteristic 2H peaks (E^1_{2g} - and A_{1g} – peak) are visible in the Raman spectra for both substrates. After the intercalation of the samples with lithium for 48 hours, both E^1_{2g} - and A_{1g} – peaks disappear in the Raman spectra, indicating the phase transformation from the 2H to the 1T phase.

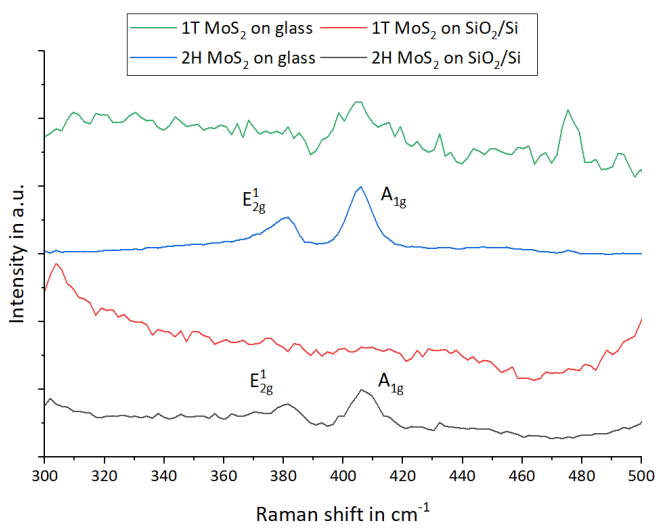

Fig. 1. Example Raman spectra of the pristine 2H MoS_2 film on SiO_2/Si and glass substrate with the two characteristic Raman peaks E^1_{2g} - and A_{1g}. After the lithium intercalation both Raman peaks have declined and can not be observed in the Raman spectrum, indicating a successful phase transition in the 1T MoS_2 phase.

The first processing result of the 1T MoS_2 film on glass substrate under ambient atmosphere can be seen in Figure 2a. The brighter lines of the letter A are the scanning path of the laser beam and the darker areas between the outlines are the 1T MoS_2 film. Around the letter a crystal growth appeared. Raman spectra of the respective areas show that the laser processing retransformed the 1T phase to the 2H phase as can be seen in Fig. 2b. The Raman spectra of the visible dark spots indicate an oxidation of the film resulting in the formation of MoO_x crystals. As a result, the experiments were reproduced in argon atmosphere, to prevent the films from oxidation, resulting in a processed MoS_2 films without a crystal growth, see Fig 83a.

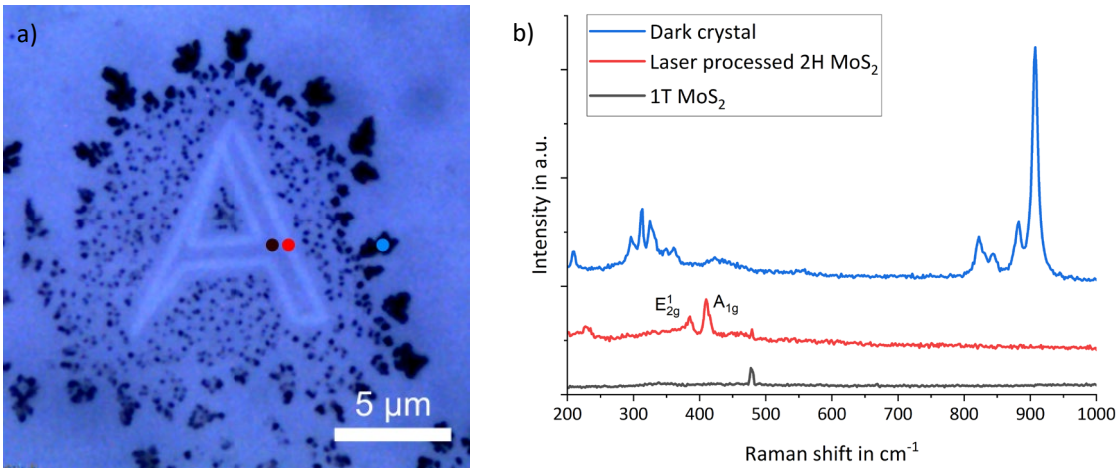

Fig. 2. (a) Light microscopy image of a laser induced phase transition on a 1T MoS_2 film on glass substrate under ambient atmosphere. The coloured spots mark the measurement spot of the Raman measurements; (b) Raman spectra of the different phases and materials that have formed during the laser processing under natural atmosphere. The laser processed area (red spot) shows the characteristic E^1_{2g} - and A_{1g} – peaks of the 2H phase, where in the unprocessed area (black spot) these peaks are missing. The Raman spectrum of the dark crystal (blue spot) shows Raman peaks, that can be associated to MoOx.

For the study of retransformation 250 µm x 250 µm rectangles were processed under Ar atmosphere on the 1T MoS_2 samples. The average laser fluence ranges from $F_{P,min}$ = 9.3 mJ/cm² to $F_{P,max}$ = 166.7 mJ/cm² with scanning speeds ranging from $v_{scan,min}$ = 1 mm/s to $v_{scan,max}$ = 500 mm/s, see Figure 3a. The first color transformation in the 1T MoS_2 film appears with a laser fluence F_P = 37.0 mJ/cm²and a scan speed v_{scan} = 1 mm/s. For higher laser fluences and scan speeds up to v_{scan} = 5 mm/s the modifications appear to get brighter, whereas the modification turns darker for even higher laser fluences and higher scan speeds then v_{scan} = 10 mm/s.

The characterization of the successful phase transformation is performed by Raman spectroscopy. Figure 3 b shows a mapping of the Raman intensity of the A_{1g} – peak depending on the laser fluence and the scanning speed for the glass substrate. The diagram shows that the intensity starts to rise at F_P = 37.0 mJ/cm² and v_{scan} = 1 mm/s (F_P = 18.5 mJ/cm² for the SiO_2/Si substrate), reaching a maximum at F_P = 74.1 mJ/cm² (F_P = 37.0 mJ/cm² for the SiO_2/Si substrate). These high Raman intensities appear in the bright modification areas, see Figure 3 a). This indicates the successful phase transition from the 1T to the 2H phase. A further rise of the laser fluence results in a decrease of the peak intensity. Due to the higher laser fluences an ablation of the film starts, resulting in the decline of the peak intensities and the darker modification in the light microscopy image. In comparison between the two substrates the laser fluence window (ΔF_p = 18.5 – 37 mJ/cm²) for the phase transformation on the SiO_2/Si substrate is lower, than the transformation window on the glass substrate. This could be induced by a different reflectivity of the substrates. For the glass substrate AF32® eco a transmission T = 0.921 is specified (Schott GmbH 2022), resulting in a maximum reflectance of R = 0.079. After Malitson (1965) the reflectance for SiO_2 at a wavelength of λ = 1030 nm is R = 0.034 and the reflectance for Si is R = 0.316 (Schinke et al. 2015). This comparison shows that the reflectance of the Si substrate is higher by a factor of four compared to the glass substrate. The reflected laser light, passing through the SiO_2 film into the MoS_2 film, can add to the transformation process, resulting in the different laser fluence requirements. A similar influence was observed by Solomon et al. 2022 during the ablation of MoS_2 on different substrates.

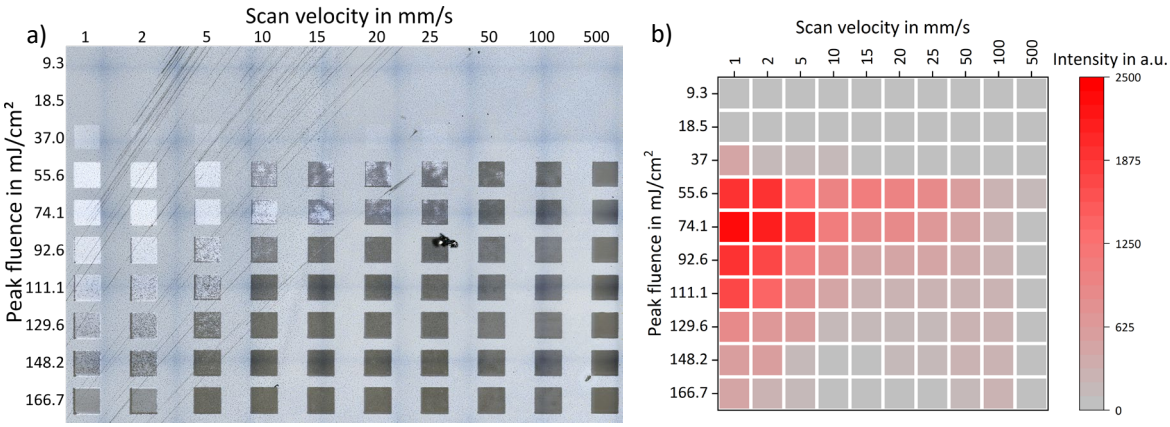

Fig. 3 Light microscope image (a) and Raman mapping of the intensity of the A_{1g} – peak; (b) of the laser processed MoS_2 film on the glass substrate. The light microscope image shows a colour modification of the 1T MoS_2 film starting at a fluence of F_P = 37 mJ/cm². For slow scan speeds (v_{scan}= 1 – 5 mm/s) a brighter modification appears, that remains until a laser fluence of F_P = 111.1 mJ/cm². For higher laser fluences and for faster scan speeds (with even low laser powers) a darker modification appears.

The influence of the scanning speed differs from the laser fluence influence. For a constant laser fluence the maximum intensity is reached with the slowest scan speed and declines with rising scan speeds. On the glass substrate the highest intensity is reached with a parameter combination of F_P = 74.1 mJ/cm² and v_{scan} = 1 mm/s, but even scanning speeds up to v_{scan} = 5 mm/s (for the SiO_2/Si substrates F_P = 37.0 mJ/cm² and v_{scan} = 1 mm/s – 10 mm/s), generate high intensity Raman signals. These scan speeds are 500 – 1000 times higher than the reported scan speeds of Guo et al. (2015) with a repetition rate 5 times less than those used by the group around Guo. The decline of the intensities and the darker modification in the light microscope image indicate an (partial) ablation of the MoS_2 film. Commonly the ablation process starts when the number of pulses per site increases (Mannion et al. 2004), known as the accumulation effect. The results of our experiments indicate a negative accumulation effect, which cannot explain at this stage. A possible explanation for this effect may be, that near the center of the laser spot partial re-transition, re-crystallization, modification (Becher et al. 2023, Sládek et al. 2022, Geng et al. 2022) appears, which increases either the reflectance or the ablation threshold of the film. For higher scan speeds the next pulse interacts with a pristine surface, whereas at lower scan speeds the pulse meets the modified surface and the energy remains under the ablation threshold. Partial ablation between the low and high scan speeds (v_{scan} = 10 – 25 mm/s, F_{Peak} = 55.6 mJ/cm²) could be due to fluctuations in the film properties or the pulse energy.

Sheet resistance measurements were performed to determine the functional properties of the MoS_2 films, first immediately after the deposition of the MoS_2 film, then after the transformation into the 1T phase and finally after the film was transformed back into the 2H phase. Since the contact regions should remain in the metallic 1T phase, this last step was only characterized via van der Pauw measurement. The 4PP measurement of as deposited 2H MoS_2 samples shows similar sheet resistances of 14 MΩ/square on both glass and on SiO_2/Si, implying higher conductivity of MoS_2 grown on glass due to the thinner MoS_2 layer on glass. Van der Pauw devices with conventional metal-TMDC contacts reveal slightly enhanced values by a factor of 2 which are typical as a result of slight degradation of the MoS_2 film during device preparation. After Li intercalation the determined sheet resistance increases by a factor of about 500 on glass and by about 900 on SiO_2. Results obtained by the van der Pauw method support these results. The resistance values do not drastically change after the laser retransformation. The 1T phase is expected to be metallic and should lead to lower resistance

values, which is not observed here. The increase in measured resistance could be due to topographical changes of the film during treatment with n-butyllithium or laser processing. A dewetting of the thin film in the microscopic scale leads to a significant increase in the resistance of macroscopic devices. In addition, the polycrystalline ALD films have significantly more defects compared to the single-crystalline exfoliated films used in previous studies. When exposed to chemical functional groups, the defects can act as highly reactive sites and efficiently trap various molecules during processing. The laser process additionally promotes the formation of defects and even oxidation, as mentioned above. The results suggest that improving the film quality, e.g., by annealing prior to the first phase transition, is desirable to increase the quality and stability of the film. To gain a deeper insight into the usp laser phase transformation process of ALD-deposited MoS_2 films, further studies on the topography of the films by atomic force microscopy, scanning electron microscopy and transmission electron microscopy as well as on the chemical composition of the films by Rutherford backscattering spectroscopy and X-ray photoelectron spectroscopy are required.

4. Conclusion

This work shows the successful usp laser induced phase transition of ALD deposited MoS_2 films on SiO_2/Si and glass substrate. We determined the parameters for laser fluence and scan speed for the transition with the highest 2H Raman signal and could reduce the process time with a scanning speed 500 times faster than the state-of-the-art process. During the experiments we observed an oxidation of the MoS_2 film, that could be prevent by the implantation of an inert gas atmosphere. So far, the laser process has led to increased resistance values of the MoS_2 films most likely due to a high defect density. Within one of our next studies an annealing step will be performed prior to the phase transformation to reduce a degradation of the film during processing.

Acknowledgements

The authors are grateful for funding and support from the Federal Ministry of Education and Research Germany (BMBF) BMBF-ForMikro-FlexTMDSense project, grant number 16ES1096K and the ForLab PICT2DES (grant number 16ES0941) and the Deutsche Forschungsgemeinschaft (DFG-SPP 1796) within FFlexCom (grant number BO2495-3-1).

Conflict of interest

The authors declare that the research was conducted in the absence of any commercial or financial relationships that could be construed as a potential conflict of interest.

References

Becher, M. J. M. J.; Jagosz, J.; Neubieser, R.-M.; Wree, J.-L.; Devi, A.; Michel, M.; Gruverich, E. L and Ostendorf, A. (2023). Ultrashort pulse laser annealing of amorphous atomic layer deposited MoS_2 films *Submitted, ArXiv:*.doi:10.48550/arXiv.2305.11008

Fan, Xiaobin; Xu, Pengtao; Zhou, Dekai; Sun, Yifan; Li, Yuguang C.; Nguyen, Minh An T.; Terrones, Mauricio; Mallouk, Thomas E., 2015. Fast and Efficient Preparation of Exfoliated 2H MoS_2 Nanosheets by Sonication-Assisted Lithium Intercalation and Infrared Laser-Induced 1T to 2H Phase Reversion, in *"Nano letters"* 15 (9) p. 5956-5960

Geng, J.; Yan, W.; Shi, L. and Qiu, M. 2022. Surface plasmons interference nanogratings: wafer-scale laser direct structuring in seconds. in "*Light Sci. Appl.*" 11, 1 – 8

Guo, Yinsheng; Sun, Dezheng; Ouyang, Bin; Raja, Archana; Song, Jun; Heinz, Tony F.; Brus, Louis E., 2015. Probing the Dynamics of the Metallic-to-Semiconducting Structural Phase Transformation in MoS_2 Crystals, in *"Nano letters"* 15(8) p.5081-5088

Huang, H. H.; Fan, Xiaofeng; Singh, David J. and Zheng, W. T. 2020. Recent progress of TMD nanomaterials: phase transitions and applications, in "*Nanoscale*" 12, 3, 1247-1268

Jagosz, J. ; Willeke, L.; Becher, M.; Ostendorf, A.; Plate, P. and Bock, C., 2022. Large-area deposition of thin crystalline MoS_2 films on 200 mm wafers using plasma-assisted atomic layer deposition, in "*Mikro-Nano-Integration; 9. GMM-Workshop"* pp. 1-4.

Kappera, R. ; Voiry, D. ; Yalcin, S. E. ; Branch, B. ; Gupta, G. ; Mohite, A. D. and Chhowalla, M., 2014 Phase-engineered low-resistance contacts for ultrathin MoS_2 transistors, in *"nature materials"* Vol. 13, p. 1128-1134

Malitson, I. H, 1965. Interspecimen comparison of the refractive index of fused silica, in "*J. Opt. Soc. Am.*" 55, 1205-1208

Mannion, P.; Magee, J.; Coyne, E.; OConnor, G. and Glynn, T. 2004. The effect of damage accumulation behaviour on ablation thresholds and damage morphology in ultrafast laser micro-machining of common metals in air. In "*Applied Surface Science*" 233, 275 – 287.

McDonell, S. ; Smyth, C. ; Hinkle, C. L. ; Wallace, R. M., 2016, MoS_2-Titanium Contact Interface Reactions, in ACS Appl. Mater. Interfaces 2016, 8, 8289−8294

Neubieser, R.-M.; Wree, J.-L.; Jagosz, J.; Becher, M.; Ostendorf, A.; Devi, A.; Bock, C.; Michel, M.; Grabmaier, A., 2022. Low-temperature ALD process development of 200 mm wafer-scale MoS_2 for gas sensing application, in *"Micro and Nano Engineering"* 15, p. 100126

Novoselov, K. S.; Geim, A. K.; Morozov, S. V.; Jiang, D.; Zhang, Y.; Dubonos, S. V.; Grigorieva, V.; Firsov, A.A., 2004. Electric field effect in atomically thin carbon films, in *"Science"* 306 (5696), p. 666–669

Novoselov, K. S.; Mishchenko, A.; Carvalho, A.; Castro Neto, A. H., 2016. 2D materials and van der Waals heterostructures, in "*Science"* 353 (6298), p. aac9439

Papadopoulos, Nikos; Island, Joshua O.; van der Zant, Herre S. J.; Steele, Gary A., 2018. Investigating Laser-Induced Phase Engineering in MoS_2 Transistors, in *„IEEE Trans. Electron Devices"*, 65 (10) p. 4053-4058

Py, M. A. and Haering, R. R. 1983. Structural destabilization induced by lithium intercalation in MoS_2 and related compounds, in "Can. J. Phys." 61, 1, 76-84

Schulmann, D. S. ; Arnold, A. J. ; Das, S., 2018, Contact Engineering for 2D materials and devices, in Chem. Soc. Rev., 2018, 47, 3037

Schott GmbH, 2022. SCHOTT AF 32® eco The alkali free answer to high technical demands, https://www.schott.com/en-hr/products/af-32-eco-p1000308

Schinke, C.; Peest, P. C.; Schmidt, J. ; Brendel, R. ; Bothe, K.; Vogt, M. R. ; Kröger, I.; Winter, S.; Schirmacher, A.; Lim, S.; Nguyen, H. T.; and MacDonald D., 2015. Uncertainty analysis for the coefficient of band-to-band absorption of crystalline silicon, in "*AIP Advances*" 5, 67168

Solmon, J. M.; Ahmad, S. I.; Dave, A.; Lu, L.-S.; Hadavand-Mirzaee, F.; Lin, S.-C.; Chen, S.-H.; Luo, C.-W.; Chang, W.-H.and Her, T.-H., 2022. Ultrafast laser ablation, intrinsic threshold, and nanopatterning of monolayer molybdenum disulfide, in "Scientific Reports" 12, 6910

Sládek, J.; Levy, Y.; Derrien, T.-Y.; Bryknar, Z. and Bulgakova, N. M. 2022. Silicon surface patterning by regular stripes of laser-induced periodic surface structures. In *„Applied Surface Science*" 605, 154664.

Van der Pauw, L. J., 1958 A method of measuring specific resistivity and Hall effect of discs of arbitrary shape, in "*Philips Res. Repts*" 13, p. 1-9

Wang, Qing Hua; Kalantar-Zadeh, Kourosh; Kis, Andras; Coleman, Jonathan N.; Strano, Michael S., 2012. Electronics and optoelectronics of two-dimensional transition metal dichalcogenides, in *"Nature nanotechnology"* 7 (11), p. 699-712